A Mathematical Model of the Emission and Optimal Control of Photochemical Smog

Daniel Burkow[1], Christina Duron[2], Kathryn Heal[3], Arturo Vargas[4]
Luis Melara[5]

August 2, 2011

Arizona State University[1], Swarthmore College[2], University of California Los Angeles[3],
University of California Irvine[4], Shippensburg University[5]

Abstract

This study models traffic regulations as well as vehicle modifications as tools for reducing the emission of NO, NO_2, CO, and CO_2 from vehicles on a subset of highways in the Los Angeles basin. We make changes to an established chemical network creating a simplified, non-autonomous, coupled set of six ordinary differential equations. We demonstrate, and prove when able, the existence of periodic pollutant levels. Furthermore, we formulate an optimal control problem to address hypothetical pollution policies explicitly considering implementation cost and the reduction of cost of adverse health effects.

1 Introduction

The geographical characteristics of the Los Angeles basin, combined with the mass amounts of daily commuters, plague the area with an accumulation of airborne chemical pollutants. These particles can be particularly harmful to the environment; carbon dioxide contributes heavily to global warming, and an increased exposure to photochemical smog is known to cause various ailments in humans, [15].

Airborne pollutant levels are especially high in Los Angeles because the region has certain geographical features that tend to "trap" air and its particulate matter close to the ground, [20]. The basin is structured in such a way that temperature inversions occur regularly. A warm air pocket accumulates above the basin and keeps cooler air (including pollutants) closer to the ground, [2]. This causes the air beneath the warm pocket to stagnate at times, an effect which is exacerbated by the mountains that frame the basin, [29]. In the warmest summer months, the temperature inversions can happen as frequently as 80% of the time, [2]. These inversions happen mostly on warm, sunny days in summer and winter, where skies are relatively clear.

Temperature inversions hold in the wide variety of chemicals that are emitted by this industrial city. Being the second most populated city in the United States, Los Angeles has a considerable amount of vehicular commuters. Combustion engines release carbon monoxide, nitric oxide and nitrogen dioxide, and are principal contributors to the formation of photochemical smog, [46]. In 1990 the EPA enacted the Clean Air Act, [13], which in part requires vehicles to be equipped with catalytic converters, [44]. This legislative action was an effort to reduce the carbon monoxide and nitric oxide emitted by a vehicular engine. While catalytic converters do reduce emission of these types, an unfortunate by-product is that they convert the molecules into carbon dioxide, which we know to be a source of other environmental concern, [22].

The combination of these phenomena over the past few decades has resulted in photochemical smog reaching critical levels in Los Angeles. Not only does smog distract from the natural beauty of the area, it is also known to cause various ailments in humans, including respiratory distress and birth defects [30]. Modeling the formation of this smog and applying hypothetical solutions to that model may help us find ways to alleviate the current pollution crisis in Los Angeles.

Models on the creation, dispersion, and interaction between the chemical components of photochemical smog have been studied since the 1950s, [27, 39, 43]. Our models expand on the work of Seinfeld et al, [43]. This earlier work focuses on the intricate kinetic processes that drive the interactions between chemicals in the atmosphere. He condensed a system of 81 chemical reactions into a simplified system with 19 reactions, [39] by averaging the reaction rates of various hydrocarbon reactions and introducing a faux chemical species (HC) to replace a majority of those reactions. Seinfeld also used partial differential equations to model the flow and dissipation of pollutants throughout the Los Angeles basin, [43]. His work deals with the mechanism behind the chemical reactions as well as the emission and dissipation of pollutant molecules. The models in his studies are so complex and interconnected that little more than graphical analysis and interpretation can be concluded.

Past optimal control models on pollution have been presented in two principal categories: vehicular emissions, [44, 48] and pollution due to point sources, [1]. Articles on optimal control of emissions from vehicles generally focus on control and implementation of more efficient mechanics, such as improved catalytic converters, [44] and spark plug placement, [48]. These controls affect the emission rate of particular chemicals from the exhaust. Other studies on pollution management focus on optimizing the emission of pollutants from factories and other similar point source emitters, [29, 51].

There has been little information on optimizing pollution emission by coupling chem-

ical kinetics models with vehicular emission sources. In our study, we analyze a non-autonomous model of ordinary differential equations, accounting for emission sources and parameterized dissipation terms. We do not explicitly consider spatial factors – such as diffusion – in an effort to simplify our model. Although possible, optimal control is difficult in the PDE setting, [3]. The model that we use allows us to optimize the emission rates of vehicles while acknowledging the chemical kinetics behind the formation of photochemical smog, [15].

In order to reduce chemical emissions, we discuss possible policy changes and also consider the cost of such strategies. By analyzing the most cost-effective policies, we are able to provide the most fitting solutions that minimize both emission levels and economic costs. We propose a policy to reduce vehicular photochemical smog emissions, consisting of direct modifications to the vehicles themselves, ideally performed on new cars by automobile manufacturers. Vehicle modifications can also include the addition of catalytic converters, the development of hybrid and fuel-cell vehicles, [41], but in this study we focus on the infusion of ethanol with unleaded gasoline.

2 Photochemical Smog

Although composed of 78.08% nitrogen, 20.95% oxygen, 0.93% argon, 0.03% carbon dioxide, and less than 4% water vapor, the Earth's atmosphere also contains minute amounts of nearly forty other gases such as ozone, helium, hydrogen, nitrogen oxides, and sulfur dioxides, [46]. These gasses are typically present in small amounts, but when their concentrations increase (due to photochemical processes and emissions) the air becomes progressively more toxic, [25].

Photochemical smog arises mostly from the combustion process of motor vehicles. This type of air pollution is produced when sunlight interacts with motor vehicle exhaust gases,

such as nitrogen oxides, to form harmful substances, namely peroxyacetyl nitrates (PAN) and ground level ozone (O_3). When present in small amounts, these pollutants pose little threat. Unfortunately, since it has been determined that ozone constitutes around 90% of smog in urban locations, photochemical smog is cause for concern, [46].

At high temperatures in the vehicle's combustion chamber, nitrogen (N_2) and oxygen (O_2) react, [2] to form nitric oxide (NO) . Once emitted into the atmosphere, some of the nitric oxide reacts with oxygen to form nitrogen dioxide (NO_2). The nitrogen dioxide reacts with sunlight, if present, which causes an oxygen atom (O) to split off. The single oxygen atom reacts with the oxygen in the air to produce ozone (O_3). Nitrogen oxide then reacts with the ozone to form nitrogen dioxide and oxygen, [15]. If the ratio of nitrogen dioxide to nitrogen is greater than three, the formation of ozone is the dominant reaction; if it is less than 0.3, the nitric oxide reaction destroys the ozone at the same rate as it is formed, thereby keeping the ozone concentration below harmful levels, otherwise the reactions tend to be balanced, [49].

Table 1 presents the reactions that we simulate in the model. There are 15 reactions with 18 chemical species, [43]. We have simplified this model into a system of six non-autonomous ODEs.

Due to the generalized nature of the model, some of the rate constants are created by necessity to make the model work, namely those specified for reactions, [6], [12], [13], [15], and [17]; the others were taken from literature. Their values are listed in Table 2.

2.1 Health Effects and Their Economic Impact

Air pollution has both acute and chronic effects on public health, [30]. These consequences depend on several variables, such as the pollutant type and its concentration in the air, as well as the individual's susceptibility and length of exposure. Ground level ozone (O_3) has been shown to cause ailments ranging from minor irritation of the eyes and the upper

respiratory system to chronic respiratory disease, heart disease, lung cancer, and death, [30]. Nitrogen oxides (NO_x) are essential ingredients in producing ground level ozone, [15], so it follows that lowering the amounts of NO_x emissions would reduce the production of O_3, resulting in fewer concerns.

2.1.1 Quantifying Health Effects

According to California Air Resources Board estimates, air pollution is associated with 19,000 premature deaths per year, 280,000 annual cases of asthma symptoms, 1.9 million lost work days per year, and more than 1 million respiratory-related school absences, [8]. Because the financial impact of breathing polluted air is staggering, we decided to focus solely on the pollution-related medical spending, such as doctor visits, respiratory and cardiovascular causes, and other medical care, that resulted from air pollution. Other medical costs, including premature mortality, lost school/work days, and asthma attacks, as well as unquantifiable factors, including time travelled and personal inconvenience, were not considered.

According to a recent RAND Institute study, Los Angeles houses over one-third of total hospitalizations related to air pollution in California. Had California met federal air standards, they concluded that an estimated 14,904 hospital admissions and emergency room visits per year would have been prevented, as well as reduction of $58,268,883 in total hospital care spending due to excessive ozone levels alone, [40].

3 Model

The mathematical models we use are based on a set of chemical reactions which are enumerated in Table 1 in the appendix. Each reaction takes on a simple form that follows $A+B \xrightarrow{k} C+D$ where A, B, C, and D are each chemical species in the reaction. Chemicals

A and B are called the reactants as they interact to form C and D, the products, at a rate k. Because these kinetics are simply rates of change, the reactions can be reformed and studied as a set of mass action differential equations, [45].

The chemical species that we study are given in terms of concentration. Due to the large scale of the environment this study is interested in, we choose to use ppm (parts per million) as a concentration ratio for each species compared to the total number of molecules in the environment. For our conversions from grams to ppm, we used 1.3×10^{13} liters as the volume of our affected region of atmosphere. To calculate this volume we multiplied the total ground area of our ten freeways (26,341,864 square meters) by the minimum height of the inversion layer and smog pillar (500 meters), which gave us a rough estimate of the volume of the tropospheric atmosphere surrounding those freeways. The concentration, ppm, is a dimensionless unit that refers to molecules per million molecules, or liters of molecules per million liters of molecules. The notation used is conventional: the concentration of chemical species, A, in the environment is given as [A].

3.1 Kinetic Mechanism

The chemical reactions are broken down into a set of ordinary differential equations for each chemical species in the system. This is achieved in a straight forward manner: each set of reactants reacts to form products at a rate of k_i in relationship to the concentration of each reactant. Consider the following:

$$\begin{aligned} A + B &\overset{k_1}{\rightarrow} C, \\ C + D &\overset{k_2}{\rightarrow} 3A, \end{aligned}$$

A and B react together at a rate of k_1 to form C. This means that we consider a mass action expression for the first reaction, $[\dot{C}] = k_1[A][B]$, $[\dot{A}] = -k_1[A][B]$, and $[\dot{B}] = -k_1[A][B]$. In the same fashion, we consider the second reaction where $[\dot{C}] =$

$-k_2[C][D]$, $[\dot{D}] = -k_2[C][D]$, and $[\dot{A}] = 3k_2[C][D]$. Combining the two sets of equations yields the following system:

$$\begin{aligned}
[\dot{A}] &= -k_1[A][B] + 3k_2[C][D] \\
[\dot{B}] &= -k_1[A][B] \\
[\dot{C}] &= k_1[A][B] - k_2[C][D] \\
[\dot{D}] &= -k_2[C][D]
\end{aligned}$$

In addition to the chemical reactions that are occurring in the atmosphere, there are two key processes that are driving the dynamics: pollution sources and sinks. For sources, we focus on that caused by traffic on ten principal freeways in the Los Angeles basin: Interstates 5, 10, 105, 110, 210, 405, 605, 710, and Routes 60 and 101. We define $f(t)$ as the total miles traveled at time t (i.e. if $t = 0$ corresponds to midnight Monday then $f(10)$ is the total number of miles being driven by traffic on all ten of the aforementioned freeways, from the hours 10AM - 11AM). The data for this project came about from the California Department of Transportation, [5]. The function $f(t)$ is a piecewise function with hour-long steps, where each level step corresponds to the average number of miles traveled during that hour. According to the EPA [14], for each mile traveled, the typical vehicle produces an average of 715 pounds of CO, 13,743 pounds of CO_2, and 47 pounds of NO_x per year. Thus, we denote the total amount of pollutant X via $\alpha_X f(t)$ where α_X is the amount of pollutant X produced per mile traveled.

The equations for $[NO], [NO_2], [CO]$, and $[CO_2]$ take on the form

$$[\dot{X_j}] = \alpha_{X_j} f(t) + R_{X_j}([\mathbf{X}], t) \tag{1}$$

where $\mathbf{X}$ is the vector of all chemical species and R_{X_j} is the difference between the sum of all reactions for which X_j is a product and the sum of all reactions for which X_j is a reactant.

Previously studied to some degree by Seinfeld, [43], the chemical reactions have created a 15 dimensional nonlinear, non-autonomous system of differential equations that also exhibit stiff dynamics, [53] due to the vast differences between various rate constants that must be studied by a stiff ODE solver (specifically ode23s in Matlab). Namely, we have processes whose rates range from $O(10^3)$ to $O(10^6)$, while others are $O(10^{-3})$. Time and resource constraints have necessitated a further simplification of the dynamics.

3.1.1 A Quasi Steady-State Simplification

To reduce the complexity of the system in Table 1, we focused on the chemicals $[NO]$, $[NO_2]$, $[CO]$, $[CO_2]$, $[O_3]$, and $[NO_3]$. The quasi steady-state assumption allows us to simplify our system by making the following observations: chemical reactions with very fast rates essentially do not change the concentration of the reactants during the course of an hour, [42]. For example, O reacts with a catalyst, M, and O_2 to form O_3 at a rate of six orders of magnitude. Therefore, when monoatomic oxygen (O) is formed, it reacts and is removed very quickly. All reactions with rates of greater **than two orders of magnitude** are considered "fast" and the associated differential equation can then be solved explicitly by setting $[\dot{X}] = \mathbf{R(X)} = 0$, where $\mathbf{R(X)}$ is some coupled autonomous equation.

Reactions with reasonably similar rates of production and removal for any initial condition can be considered at a steady state and then solved in a similar fashion. We do not explicitly consider nitric acid ($[HNO_3]$) and polyacrylonitrile ($[PAN]$) since they are "sinks" (i.e. their associated ODE's are strictly positive and are not reactants in any process). We further assume that the concentration of oxygen ($[O_2]$) is constant, denoted by $\overline{[O_2]} = 209460\ ppm$, since any impact of a less abundant chemical on the concentration of oxygen would be insignificant. The ODEs for $[HC]$ and $[RO_2]$ are removed from the system since we will not consider the effects of hydrocarbons in this model. If $[\dot{HC}]$ and $[HC]_0$ are both zero, then there is no $[RO_2]$ production, which means the ODEs can be

ignored. We chose to exclude hydrocarbons $[HC]$ and $[RO_2]$ as the former is the main proponent of stiff dynamics and the latter was the primary product of $[HC]$ interactions. A difficulty with excluding $[RO_2]$ is that it reacts with $[NO]$ to create $[NO_2]$ and a small amount of $[OH]$ radicals. Thus we can expect the $[NO]$ generated from our approximation to be larger than measured levels and $[NO_2]$ to be lower. Excluding the $[HC]$ dynamics will result in our model predicting higher levels of ozone.

We found that $[OH]$ has a fairly constant nominal value and thus, we assume OH as constant and denoted by $\overline{[OH]} = .0000001\ ppm$, [37]. $[HO_2]$ is excluded through a similar assumption, however in this case, we solved for when $[\dot{HO_2}] = 0$, and thus solving for $[HO_2]^*$, getting:

$$[HO_2]^* = \frac{k_8[CO]\overline{[OH]}}{k_9[NO] + k_{10}[NO_2]}.$$

The exclusion of $[O]$ is done in a typical quasi steady state manner, as the reaction rate of $[O]$ with $[O_2]$ is 2.76×10^6 and with $[RO_2]$ is 7300, thus $[O]$ is a fast dynamic. Therefore, we assume $[O]$ has attained equilibrium and obtain:

$$[O]^* = \frac{k_1 h(t)}{k_2} \frac{[NO_2]}{\overline{[O_2]}}.$$

where $h(t)$ is a dependency on sunlight intensity.

The justification for the exclusion of $[HNO_2]$ is perhaps the weakest at this point because the reaction rates are not especially large, but create similar in and out flows. We assume a relatively constant amount and solve for the relational solution explicitly:

$$[HNO_2]^* = \frac{h(t)k_7}{2k_6[NO][NO_2]}.$$

Although there exist various removal mechanisms for tropospheric pollutants, including vegetation and soil, we will focus solely on the winds that affect our freeway regions.

3.1.2 Wind

Accumulation of chemicals within the system is inevitable without a removal mechanism such as wind. Wind is calculated in the model by a very simplified rate constant as opposed to a system of spatial equations due to our small area of interest immediately surrounding the set of freeways. We found an average constant 6.6 $\frac{mi}{hr}$ wind speed, the minimum time over which a particle can travel across the freeway and that any emitted particle immediately takes on the speed of its surrounding particles. To do this, the average east-west distance (in miles) across any one of the freeways is determined by calculating the approximate angle of each freeway's orientation away from north-south between $0°$ and $90°$ as well as the percentage of total freeway length each individual freeway encompasses. The relative angle, θ is used to find the East-West distance across the freeway using, $a \cdot sin(\theta) + b$ where a and b are constants such that $a \cdot sin(0°) + b = b = Width_{avg}$ and $a \cdot sin(90°) + b = a + b = Length_{avg}$, where the $Length_{avg}$ and $Width_{avg}$ are the average length and width of all ten freeways. The resulting distances are multiplied by the percentage length of each freeway and all of these values are summed. The average wind speed (6.6 $\frac{mi}{hr}$) is divided by the average distance value to give a rate of 135.9 hr^{-1}. This is the rate it takes for a particle to travel across the entire average east-west cross section of freeways at a constant 6.6 $\frac{mi}{hr}$. This rate is represented by w in the models, and is referenced in each differential equation $[\dot{x}]$ as a part of the term $w([x]_0 - [x])$. Pollutants are emitted over a wide range of locations within the freeway system, which creates some error within the model.

3.1.3 Chemical Sinks

Chemical sinks absorb or modify a chemical without being involved in any other process within the system. We ignore chemical sinks in our model due to two major considerations.

Elements such as vegetation and soil are natural sinks for CO_2 and CO, respectively. On the other hand, soil is a natural source of CO_2 emission and vegetation only absorbs CO_2 during the daytime, emitting CO_2 via respiration at night. Therefore, due to the complex nature of the natural CO_2 cycle and the significantly low effect it has on a small geographic scale, vegetation is not considered as a chemical sink within our system. Then, for CO, we considered an area 10% larger than the area of roadway that the freeways encompass, and approximated the percentage of the area composed of soil. The area of soil was multiplied by the rate at which soil absorbs CO per hour, [21], at a temperature of 30 °C which yielded a rate of .0001hr^{-1} which is negligible in our system, and is therefore ignored.

3.1.4 Solar Intensity

Photochemical smog relies on sunlight for chemical reactions to occur. Photons emitted from the sun travel at various wavelengths and intensities and as they pass through the atmosphere, the photons interact with airborne molecules. The absorbed photons increase the energy within the absorbing molecule and cause electrons to become excited. The result is either the emission of another, lower frequency photon due to the excited electron dropping down an energy level, or a chemical change to the structure of the molecule itself. For photochemical smog, the chemical change we are interested in is called photolysis, which is the splitting apart of a molecule due to the absorption of photon energy. The rate at which a molecule dissociates is related to the quantum yield (the number of dissociations per absorbed photon) multiplied by the physical cross section of the molecule being studied and adjusted by the intensity and wavelength of the photons being absorbed, [27]. A simple model considers the seasonal periodic zenith angle of the sun in addition to daily sunrise and sunset.

The intensity of sunlight that reaches earth's surface (measured by units of photons cm^{-2} s^{-1} called the actinic flux) is affected heavily by two key factors. First, the angle of

the sun in accordance to the plane of earth on which we study these reactions very strongly affects the intensity of the solar energy, [35]. The noontime zenith angle of the sun changes over the course of a year due to the earth's tilt in relationship to its revolution around the sun, which is the cause for seasonal temperature fluctuation. Second, the density of atmosphere through which the sunlight must travel as well as meteorological effects such as clouds heavily influence the magnitude of the actinic flux. In general, about 50% of the actinic flux that penetrates the atmosphere makes it to the surface of earth and decreases dramatically with cloudy or overcast skies, [34]. Due to the variability in the number of cloudy days over the course of a year, we find it necessary to assume the extreme case of year round clear skies.

Formulating the solar intensity model is a combination of seasonal periodic sun angles and daily sunlight hours. The angle of the sun in relation to the horizon at noon (called the zenith angle) for every day in 2010 was used to develop a seasonal periodic intensity function, [50]. We took the sine of the angles in order to approximate percentage transmission. The points were fit by a Fourier series approximation which was scaled to match the 50% reduction in transmission by the meteorological effects. The sunrise and sunset times for the spring and autumnal equinoxes were averaged and used to create the daily periodic fluctuation of solar intensity which is multiplied to the seasonal intensity function creating our final solar intensity function called $h(t)$. This time dependent function scales the maximum photolysis rate of NO_2 and O_3.

The simplified system, dropping the time dependence notation in f and h and introducing a scalar term w which represents dissipation of particles due to wind, is below:

$$
\begin{aligned}
[\dot{NO}] &= \alpha_{NO} f + h \cdot k_1[NO_2] + h \cdot k_7[HNO_2]^* - [NO](k_3[O_3] + k_6[NO_2] \qquad (2)\\
&\quad +k_9[HO_2]^*) + w([NO]_0 - [NO]),\\
[\dot{NO_2}] &= \alpha_{NO_2} f + k_3[O_3][NO] + [HO_2]^* \left(k_9[NO] - k_{10}[NO_2]\right) \qquad (3)\\
&\quad -[NO_2]\left(h \cdot k_1 + k_4[O_3] + k_6[NO] + k_5[NO_3]\right) + w([NO_2]_0 - [NO_2]),\\
[\dot{NO_3}] &= [NO_2]\left(k_4[O_3] - k_5[NO_3]\right) + w([NO_3]_0 - [NO_3]), \qquad (4)\\
[\dot{CO}] &= \alpha_{CO} f - k_8[CO]\overline{[OH]} + w([CO]_0 - [CO]), \qquad (5)\\
[\dot{CO_2}] &= \alpha_{CO_2} f + k_8[CO]\overline{[OH]} + w([CO_2]_0 - [CO_2]), \qquad (6)\\
[\dot{O_3}] &= k_2\overline{[O_2]}[O]^* - [O_3]\left(k_3[NO] + k_4[NO_2]\right) + w([O_3]_0 - [O_3]) \qquad (7)\\
[HNO_2]^* &= \frac{h(t)k_7}{2k_6[NO][NO_2]} \qquad (8)\\
[HO_2]^* &= \frac{k_8[CO]\overline{[OH]}}{k_9[NO] + k_{10}[NO_2]} \qquad (9)\\
[O]^* &= \frac{k_1 h(t)}{k_2}\frac{[NO_2]}{\overline{[O_2]}} \qquad (10)\\
\overline{[O_2]} &= 209460\ ppm \qquad (11)\\
\overline{[OH]} &= 0.0000001\ ppm, \qquad (12)
\end{aligned}
$$

where [X]* denotes QSSA and $\overline{[X]}$ a constant value.

3.2 Stability Analysis of the Non-Autonomous System

Ideally, our system of differential equations ($[NO]$, $[NO_2]$, $[NO_3]$, $[CO]$, $[CO_2]$ and $[O_3]$) would have periodic solutions. This would indicate that the behavior of each chemical would exhibit some kind of predictable behavior over time; it would not, for example, grow or decay exponentially. A periodic solution that reaches an asymptotic stability is ideal when discussing control of a system because its behavior pattern can be affected by manipulating its parameters (in our case, α_x and $f(t)$).

Of the equations above, we are able to show asymptotic stability algebraically for only $[CO]$ and $[CO_2]$. Due to the complex relationships between the remaining four compounds, we can only look at the boundaries within which solutions may exist.

3.2.1 Existence of a Periodic Solution: Carbon Monoxide

We show the existence of a periodic solution to $[\dot{CO}]$, [19]. First note that

$$[\dot{CO}] = \alpha_{CO} f(t) + w[CO]_0 - [CO]\left(k_8\overline{[OH]} + w\right)$$

taking $w = 135.9 \cdot hour^{-1}$ as our wind term and $[\mathrm{CO}]_0$ as the initial condition. We rewrite this as

$$[\dot{CO}] = g(t) - G([CO])$$

where $g(t) = \alpha_{CO} f(t) + w[CO]_0$ and $G([CO]) = [CO]\left(k_8\overline{[OH]} + w\right)$

The positive periodic function, $f(t)$, is bounded by the constants $m \sim 8.0 \cdot 10^5$ and $M \sim 5.6 \cdot 10^6$ as found by averaging yearly traffic patterns, and thus

$$(\alpha_{CO} m + w[CO]_0) - G([CO]) \geq [\dot{CO}] \geq (\alpha_{CO} M + w[CO]_0) - G([CO])$$

There exist two distinct spaces, which we denote U_+ and U_-. As t increases, a solution is increasing in U_+ and decreasing in U_-.

$$U_+ = \{(t, [CO]) : (\alpha_{CO} m + W[CO]_0) - (k_8\overline{[OH]} + w)[CO] > 0\}$$

$$U_- = \{(t, [CO]) : (\alpha_{CO} M + W[CO]_0) - (k_8\overline{[OH]} + w)[CO] < 0\}$$

The orientation of U_+ and U_- satisfies the formal criteria for existence of a periodic solution to $[\dot{CO}]$. Define

$$a_0 = \int_0^1 \left(\frac{\partial}{\partial [CO]}\left((\alpha_{CO} f(t) + w[CO]_0) - [CO](k_8\overline{[OH]} + w)\right)\right) dt \ .$$

By Theorem 4.22 from J.K. Hale's Dynamics and Bifurcations, we have that if $a_0 < 0$, the periodic solution is asymptotically stable and that if $a_0 > 0$, the solution is unstable. We have

$$a_0 = -\int_0^1 (k_8\overline{[OH]} + w)\, dt$$

$$a_0 = -(k_8\overline{[OH]} + w)$$

Because $k_8\overline{[OH]} + w$ is a positive constant term, a_0 is negative, and any periodic solution to $[\dot{CO}]$ is asymptotically stable.

3.2.2 Carbon Dioxide

We then focus on the second less coupled reaction

$$[\dot{CO_2}] = \alpha_{CO_2} f + k_8[CO]\overline{[OH]} - w[CO_2] + w[CO_2]_0$$

In lieu of including the w wind terms as we did above, we have left the carbon dioxide with a more general $w[CO_2]_0 - w[CO_2]$ term. This will not affect our determined uniqueness or stability, as the bounds will simply be shifted up or down according to the positive constant w.

We previously concluded that $[\dot{CO}]$ has periodic solutions. This means that a solution $[CO]$ is bounded by some q and Q such that $q \leq [CO] \leq Q$. Recall that the periodic miles-traveled function $f(t)$ is bounded by m and M such that $m \leq f(t) \leq M$. We use this to see that

$$m + q \leq \alpha_{CO_2} \cdot f(t) + k_8[CO]\overline{[OH]} \leq M + Q$$

then

$$m + q - w[CO_2] + w[CO_2]_0 \leq [\dot{CO_2}] \leq M + Q - w[CO_2] + w[CO_2]_0$$

In a similar process as before, we analyze the solution spaces:

$$U_+ = \{(t, [CO_2]) : m + q - w[CO_2] + w[CO_2]_0 > 0\}$$

$$U_- = \{(t, [CO_2]) : M + Q - w[CO_2] + w[CO_2]_0 < 0\}$$

The orientation of U_+ and U_- satisfies the formal criteria for existence of a periodic solution to $[\dot{CO_2}]$, [19] .

The asymptotic stability of the periodic solutions to $[\dot{CO}]$ and $[\dot{CO_2}]$ implies that over a lengthy stretch of time, as $t \to \infty$, the solution will exhibit a somewhat predictable behavior; thus, we can study long-term effects of our policies on future concentration levels in Los Angeles.

The proofs of existence, uniqueness and stability are trivial for carbon monoxide and carbon dioxide. However, the remaining four equations in our system become significantly more difficult to analyze because they are coupled in such a way that analytically defining a bounding region is difficult.

3.3 Analysis of the Non-Autonomous Model

Due to the intricacy of the coupled equations, we numerically solved the non-autonomous system for a one year period to study the dynamics. All of the minimum values of the system (except for NO_2) were the initial conditions, indicating a strong increase in concentration for the following hours. Maximum values of the equation fall beneath the EPA standards. The percentage increase from initial conditions that each pollutant displayed, as well as the annual mean and standard deviation, can be seen in Table 3.

From Table 3, CO_2 has the greatest variability in the system due to the high standard deviation even though on average, CO_2 never exceeds its initial condition (390ppm) by more than 0.17%. Also, NO has the highest percent increase from initial conditions (867%) which is interesting because, while ambient NO levels are low, vehicles emit a greater amount of NO than NO_2, and NO_2, which break down in the presence of sunlight to form NO. The numbers produced by this model are consistent with pollution level fluctuations described above, and so we can say that this model can be used as a relative

measure for policy implementation.

Graphical analysis of the system also displays behavior like that which is seen in the field. The plots of the system over time show bounded periodic behavior with seasonal and daily variation.

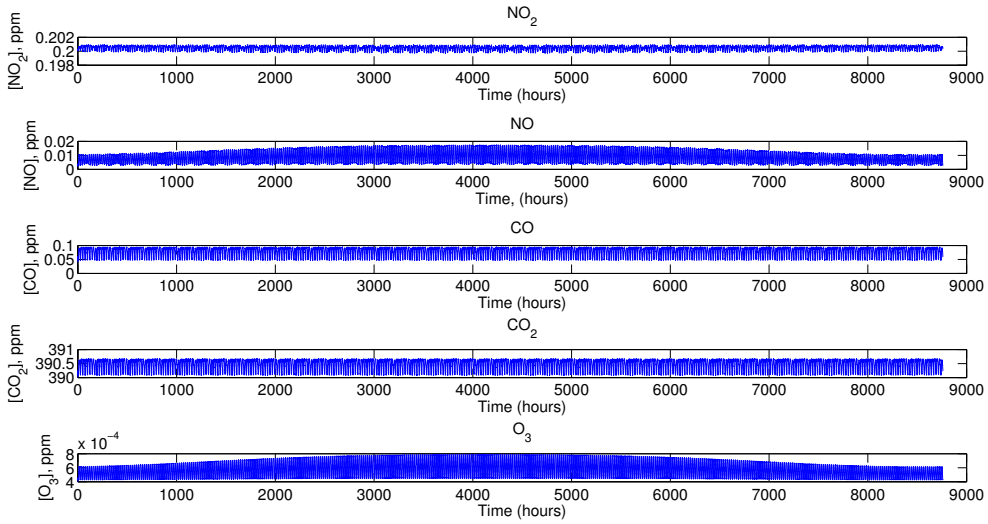

This set of plots shows the hourly fluctuation of concentration over the course of a year. The smaller details are obscured because of the relatively high frequency of the daily cycle. However, this view shows the relative change in extreme daily values as seasons go by. For a more intricate view, consider the following:

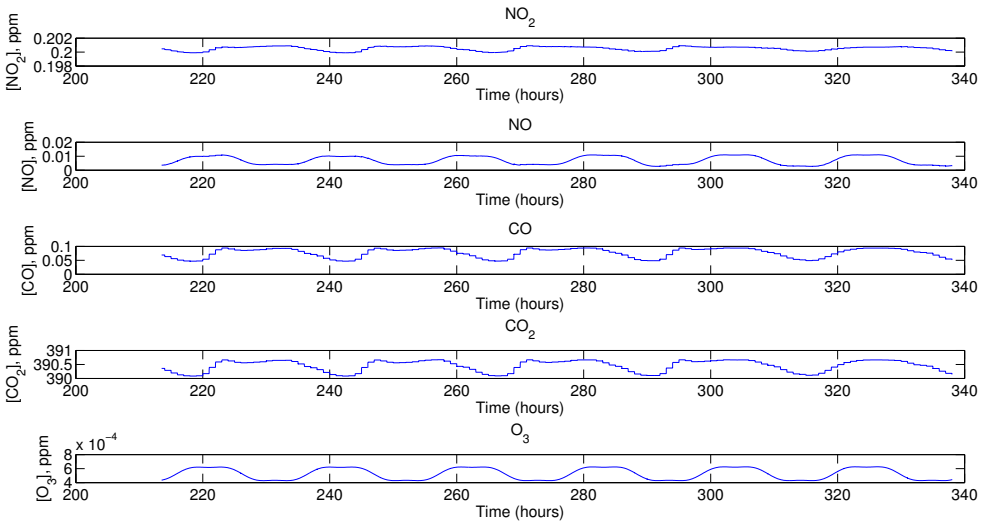

In this plot, the daily fluctuations are visible and it can be seen that the fluctuation of traffic patterns throughout the week affect the shape of the concentration of each chemical concentration plot. This mimics the physical reality of photochemical smog as pollution is highest during the day while the density of cars on the road is greater. Finally, ozone (O_3) is the highest during the peak hours of the day (for clarification, hour 240, as shown in the plot, is the end of the 10th day in our system - January 10th).

This model appears to simulate the dynamics of average periodic pollutant fluctuations. However, it fails to provide useful information on unpredictable events such as unusually dense traffic, wind variation, cloud coverage, and variation in the height of the temperature inversion layer.

3.3.1 Autonomizing the Kinetic System

To simulate the long term dynamics of the system, we autonomize the kinetic system by holding both $f(t)$ and $h(t)$ constant. This leaves us with a less complicated model through

which we can study various cases. Thus, we have:

$$\begin{aligned}
[\dot{NO_2}] &= k_3[NO][O_3] + k_9[NO][HO_2] + w[NO_2]_0 + \alpha_1 \\
&\quad -[NO_2](J_1 + k_4[O_3] + k_5[NO_3] + k_6[NO] + k_{10}[HO_2] + w), \\
[\dot{NO}] &= J_1[NO_2] + w[NO]_0 + \alpha_2 - [NO](k_3[O_3] + k_6[NO_2] + k_9[HO_2] + w) + \frac{J_2^2}{2k_6[NO_2][NO]}, \\
[\dot{O_3}] &= J_1[NO_2] + w[O_3]_0 - [O_3](k_3[NO] + k_4[NO_3] + w), \\
[\dot{NO_3}] &= k_4[NO_2][O_3] + w[NO_3]_0 - [NO_3](k_5[NO_2] + w),
\end{aligned}$$

where $\alpha_i,\ i = 1,\ 2$ are constant parameters for miles driven $\times$ emission per mile, and $J_i = h(t)k_i$, $i = 1, 2$, where $h(t)$ is the sunlight function and w is the wind constant.

We consider four extreme cases: (max{f}, max{h}), (max{f}, min{h}), (min{f}, max{h}), (min{f}, min{h}). We then take the limit of the system as $t \to \infty$ and plot the limiting values on a phase plane between two of the state variables. These points form the corners of a quadrilateral boundary within which any quasi-periodic solution from the non-autonomous system will be contained. Since the non-autonomous system behaves in a complex manner, explicit solutions cannot be obtained and so we study the boundaries within which the long term "solutions" will be contained.

As a demonstration, with the same initial conditions and rate constants, we evaluated the non-autonomous system for 1 year, producing a phase portrait of NO_2 against O_3, which is plotted in the geometrical figure with extreme stable values presented above as vertices.

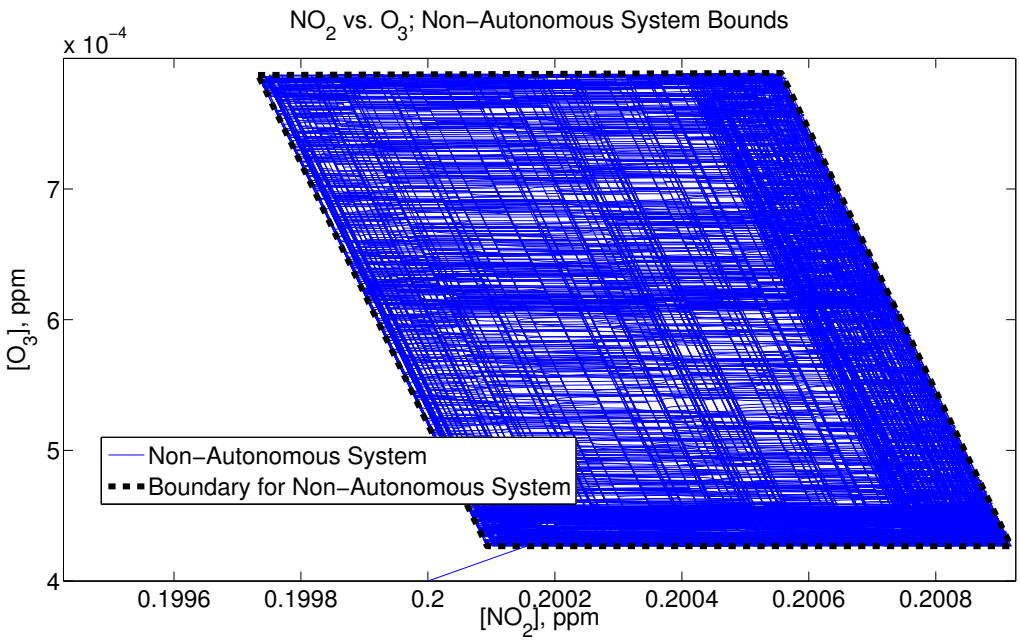

Figure 1: Non-autonomous system dynamics and bounds

It is clear that the dynamics, displayed in Figure 1, of the non-autonomous system is contained within the lines between the extreme values from the autonomous system. Therefore, the boundaries formed from the autonomous system can be used to study the change associated with the implementation of various policies. For further clarification on the behavior of the non-autonomous system during the year, we look at the first week, and the 20th week of the year.

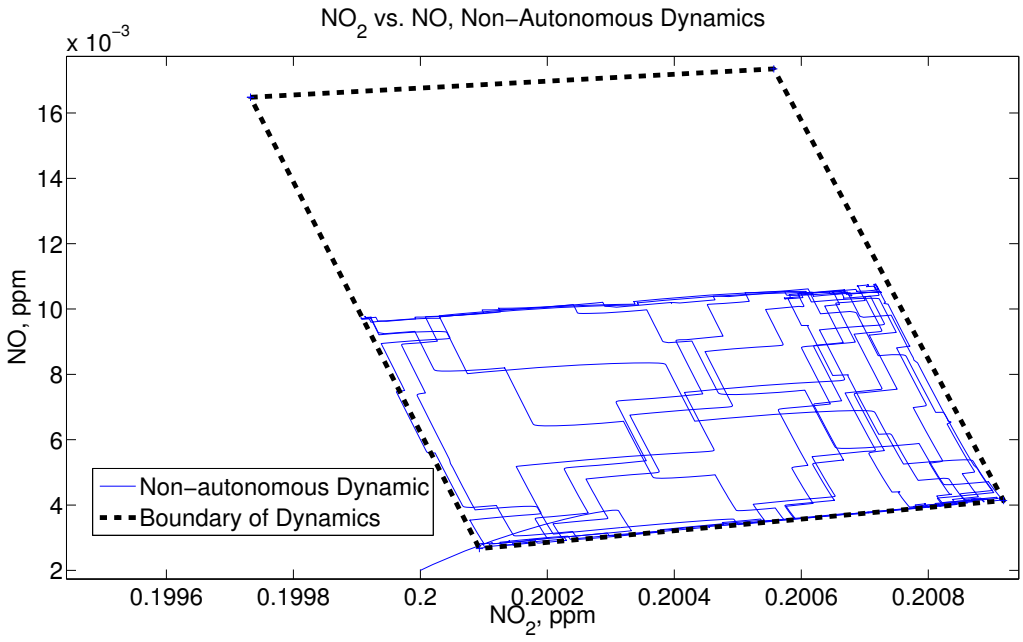

Figure 2: Evaluation of Week 1

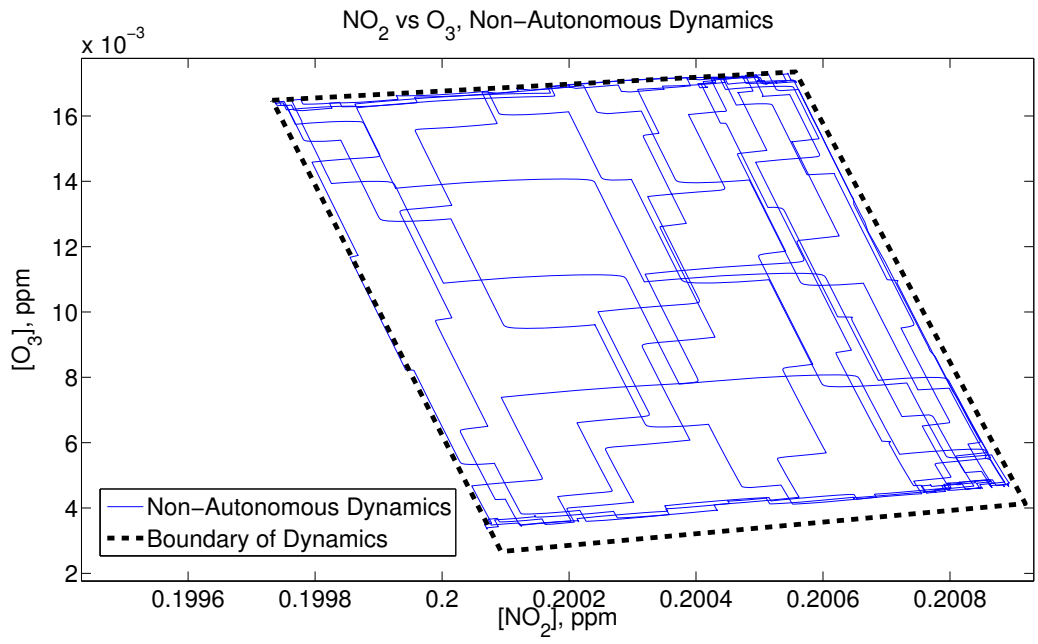

Figure 3: Evaluation of Week 20

The two single week plots show that the range of concentrations during the summer is greater than that during the winter and the maximum value of NO_2 actually occurs during the winter, indicating that with the same emission rates, the increased sun intensity breaks down the NO_2 faster. Since we focus on yearly emissions, we assume the dynamics are the edges of the geometric shape in Figure 3.

4 Policies

The state of California currently imposes an air quality standard allowing no more than 0.07 ppm ozone and 9.0 ppm carbon monoxide over any eight-hour period, [24]. From 2000 to 2007, the Los Angeles basin has exceeded this ozone standard on average 92 days per year, [24]. The policies that we propose are intended to reduce the concentration of

pollutants emitted by vehicles in order to meet this standard. We propose two methods of such a reduction: vehicular modifications and traffic regulation.

4.1 Vehicular Modification

We propose a "vehicular modification" type of policy that involves the development of ethanol-infused unleaded gasoline. This mixture of ethanol into regular petroleum gasoline has been shown to reduce greenhouse gas emissions, including the photochemical pollutants of concern. We discuss the effects of E0 (pure unleaded petroleum), E20 (a mixture of 20% ethanol and 80% petroleum), and E85 (85% ethanol and 15% petroleum).

One source of ethanol is corn, [4]. Large-scale production of corn ethanol would require sizable portions of edible corn crops to be dedicated to ethanol, which would drive the prices of food corn up and possibly require the federal government to further subsidize corn farmers as an incentive to grow corn for ethanol instead of food. Studies show that even if all corn and soybean crops were dedicated to biofuels (including those formerly used for food), they would replace only 12% of our average gasoline consumption, [4]. Furthermore, a reduction in corn feed would strain the meat industry. In addition to the agricultural effects of ethanol, the "clean" fuel is ironically dirty to produce; most of the time, ethanol plants actually burn coal to fuel the distillation process, [4]. Between the reduction in on-road emissions and cost to produce the ethanol, the pollutant savings and energy ratio appears to break even.

Ethanol can also be produced using cellulose, which includes corn stalks, leaves, sawdust and other inedible organic compounds, [4]. Cellulose is environmentally cheaper to produce and more effective at reducing pollutant emissions than corn-based ethanol, [28]. Other methods that are currently being researched include sugar cane ethanol and algae. Sugar cane ethanol has been effectively used on a smaller scale in Brazil for several years, [4]. Algae is also being investigated as a potential source, as each acre of algae may be

able to produce over 5000 gallons of biofuel each year, as opposed to 300 gallons for corn and 60 gallons for soybeans, [4].

Most vehicles manufactured before the year 2003 may not be able to run on gasoline mixtures with more than 20% ethanol unless they have been modified to accommodate such types of fuel, [28]. The number of new fuel-flexible vehicles produced grew from 40,000 in 2003 to 1.7 million in 2007. These vehicles can be purchased new at little to no additional cost from traditional fossil fuel burning vehicles, [12]. To convert older cars and trucks to run on higher-concentration ethanol mixtures, the consumer must purchase a modification kit that costs around $400, [16].

As of July 2011, the average price of regular unleaded petroleum gasoline was approximately $3.82, with E85 at an average of $3.32, [17]. Running on E85 reduces a vehicle's fuel economy by an average of 25%, [9, 12]. This means that although E85 is 13% cheaper than pure unleaded petroleum, [54], consumers would actually pay an extra $8,535,824.62 (i.e., an average of $0.33 more per gallon) for fuel over the course of a year. This figure is a sum for all drivers in Los Angeles (a fraction of the population of 9,818,605) over an entire year, and was not calculated per individual, [52]. This amount does not include the cost to modify older cars for fuel-flexibility.

The federal government would need to make a substantial financial contribution to this effort. Each gallon of petroleum that is displaced by ethanol in a gasoline blend costs the United States government $1.78 in terms of subsidies to corn farmers and lost tax revenue due to tax rebates as consumer incentives, [38]. For a year-long program, this cost adds up. For all of the ten freeways we study in Los Angeles, as in our model, we take the sum of total distances travelled to be, on average, 538,835,900 miles per year, [5]. EX denotes an ethanol mix of $X\%$ ethanol and $(100 - X)\%$ petroleum. In our calculations we use the average estimated mileage of most passenger cars and light trucks, 21.1 miles per gallon, which does not include the reduction in fuel economy due to ethanol blends,

[7]. The total annual cost to implement an EX program for all of Los Angeles for a year can be calculated using

$$\frac{538,835,900\ miles}{1\ year} \cdot \frac{1\ gallon\ EX}{21.1\ miles} \cdot \frac{X\ gallons\ ethanol}{100\ gallons\ EX} \cdot \frac{\$1.78}{1\ gallon\ ethanol}$$

which reduces to $\$454,562.99(X)$ per year for an EX program.

Applying this formula to the cases of E20 and E85 yields an extra annual cost to the federal government of $9,091,259.73 for E20 and $38,637,853.87 for E85. The combined total cost to implement an E85 program for all Los Angeles amounts to $47,173,678.49 per year, a cost that would be shared between the government and a large fraction of the city's population. We can also calculate the annual cost per car, under the assumption that all $2,499,764$ registered non-commercial vehicles in Los Angeles, [26] travel, on average, the same number of miles per year on our ten freeways of interest. Thus, we have

$$\frac{538,835,900\ miles}{2,499,764\ cars \cdot year} \cdot \frac{1\ gallon\ EX}{21.1\ miles} \cdot \frac{X\ gallons\ ethanol}{100\ gallons\ EX} \cdot \frac{\$1.78}{1\ gallon\ ethanol}$$

which reduces to $\$0.18(X)$ per car, per year, to implement EX program.

More specifically, we propose that if by January 1st of some year, $\gamma\%$ of all registered vehicles in Los Angeles are required to be running on EX fuel, then the cost of one year of this program is

$$\frac{\gamma\ cars}{100\ cars} \cdot \frac{\$0.18(X)}{car \cdot year}$$

The quantitative benefits that we use in our EX policy calculations are in terms of reduction of health care spending due to pollution-related illnesses (from chemicals like CO, O_3, and NO_2). Other benefits are long-term environmental effects such as slowing the rate of global warming due to carbon dioxide accumulation.

4.1.1 Analyzing the results for Ethanol/Petroleum mixed fuel

The ethanol mixtures E20 and E85 affect the steady emission rates of vehicles and the results of implementing such policies can be studied be altering α emission rates. Policies

are implemented by adjusting α values with non-negative scalars, where 0 is 100% reduction and 1 is 0% reduction. We then study the area of the boundary box as a relative scale for emission control. We consider the region within which the non-autonomous system is bounded as found by plotting the extreme points from our autonomized model and connecting the stable points. We have found that E20 scales CO by .89, CO_2 by .78, and NO_x by 1.02, and also that E85 scales CO by .86, CO_2 by .70, and NO_x by .90, results that are apparent in our bounding boxes.

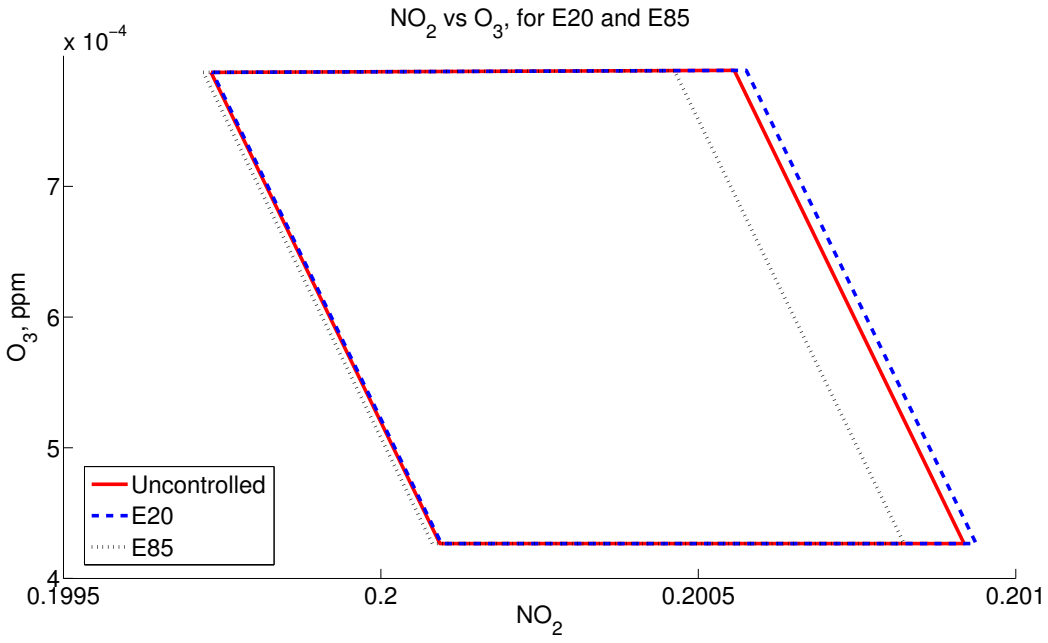

Figure 4: Comparing the Bounding Boxes for NO_2 to O_3 for fuel types E20 and E85

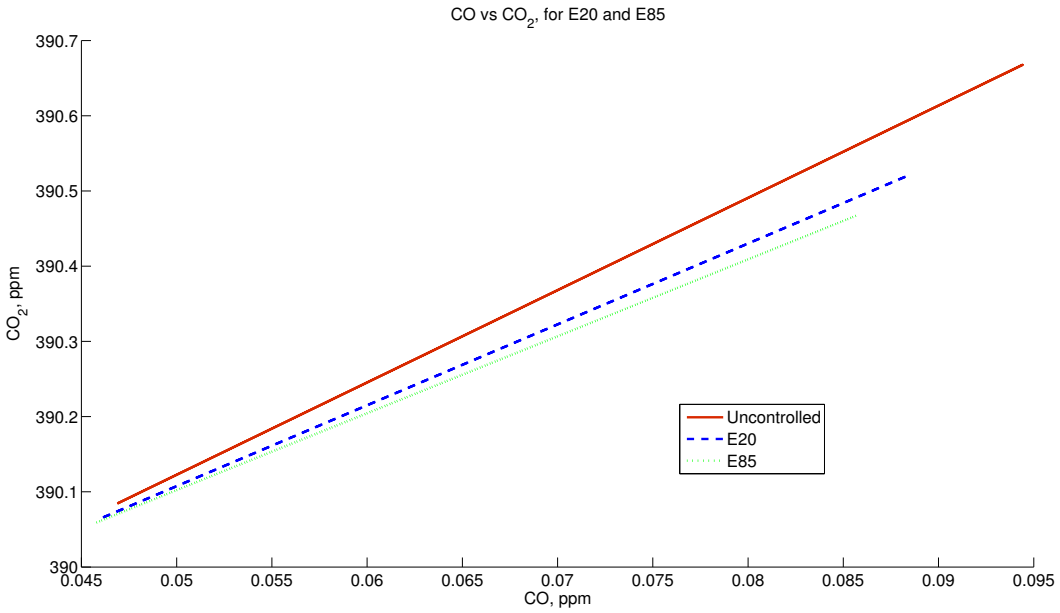

Figure 5: Comparing the Bounding Boxes for CO_2 to CO for fuel types E20 and E85; the lines show that CO_2 and CO have a nearly linear relationship.

The solutions to the non-autonomous system are contained within the boundaries of the bounding boxes as shown in Figures 4 and 5. This result is numerically uninteresting, but qualitatively demonstrates how emission controls, such as ethanol mixed fuels, affect the periodic boundaries of the non-autonomous system. We can evaluate the extreme points of the bounding boxes to determine the maximum and minimum pollutant concentration. However, we cannot extrapolate over which hours these pollutant extrema occur. Also, the behavior of the solutions of the non-autonomous system cannot be concluded from the information given by the bounding boxes.

4.2 Traffic Regulation

Stop-and-go traffic produces more pollutants than free-flow traffic, making accelerating and idling the two most polluting operations a gasoline engine can do, [32]. Reducing air pollution will require sensible and strategic changes in the transportion infrastructure, specifically targeting an alleviation of traffic congestion.

One approach to traffic reduction is through the implementation of toll roads. Despite their growing development worldwide, few tolls are utilized in the United States. In fact, having one of the nation's top economies, California has only 5 tolls that span a total of 75 miles. Yet, most roads in the United States are constructed with public funds and provided to drivers for free, [31]. Nevertheless, charging drivers a fee for use of the roads continues to be a popular suggestion to reduce traffic. Various studies have been done on toll roads that analyze their effect on traffic congestion, [32].

Prior to toll roads, the Riverside Freeway was subject to high volumes of traffic due to the few direct routes between Orange and Riverside Counties. The State Route 91 experienced traffic delays up to 40 minutes in each direction during peak traveling hours, [47]. In response, public officials constructed toll roads in the 10-mile median of the freeway. In 1995, the SR-91 Express Lanes opened as a privately funded tollway that adjusted toll rates based on peak hours. Researchers analyzed the benefit-cost of variable pricing of the SR-91 Express Lanes, studying its impact on tens of thousands of travelers, [47]. The examined benefits included travel time savings, fuel use, change in emissions, while the costs comprised of the initial investment and facility maintenance. Overall, the total discounted benefits for the 10-year study exceeded the total discounted costs by over $50 million, [47].

The International Council on Clean Transportation analyzed the potential costs and benefits of implementing toll roads with variable pricing in Santa Clara County, California, one of the ten most congested areas of the United States. They predicted a 22-million hour

per year in time-savings from avoided congestion and $250 million in gasoline savings, [36]. Furthermore, they estimated that CO_2 emissions could be reduced 17% through congestion tolls on freeways, a reduction of over 600,000 tons and savings of approximately $30 million annually, [36].

The paper in [33] estimates that passenger cars are responsible for nearly 30 percent of greenhouse gases in California. Trends have indicated that growth in vehicle miles traveled (VMT) over the next 20 years will negate the CO_2 benefits of current vehicle improvements, and so decreasing VMT is crucial to reducing air pollution, [33].

5 Optimal Control

We applied optimal control methods to our results from previous sections to determine the most cost-effective degree of policy implementation. Our goal is to minimize the amount of pollutants being emitted into the atmosphere by motor vehicles. In optimal control, ϵ is a relative cost that incorporates both a qualitative cost and benefit of the policy, in dollars.

5.1 Existence of an Optimal Control

We model the proof of existence of an optimal control scenario from a 2006 study by de Pillis, et al, [10]. Let U be the admissible control set, containing all possible control functions $u(t)$, all of which are bounded by 0 below and 1 above. In other words, given the objective function,

$$J\left(u(t)\right) = \int_0^{t_f} \left([NO] + [NO_2] + [CO] + [CO_2] + [NO_3] + [O_3] + \frac{\epsilon}{2}u(t)^2\right) dt,$$

where

$$U = \{u(t),\ \textit{piecewise continuous}, |\ 0 \leq u(t) \leq 1, \forall t \in [0, t_f]\},$$

subject to our non-linear system mentioned in a previous section, with initial conditions $[NO]_0, [NO_2]_0, [CO]_0, [CO_2]_0, [NO_3]_0$, and $[O_2]_0$ then there exists an optimal control $u^*(t)$ such that

$\min_{u(t)\in[0,1]} J(u(t)) = J(u^*(t))$ if the following conditions are met:

- The class of all initial conditions with a control $u^*(t)$ in the admissible control set along with each state equation being satisfied is not empty.
- The admissible control set U is closed and convex.
- Each right hand side of the state system is continuous, is bounded above by a sum of the bounded control and the state, and can be written as a linear function of $u^*(t)$ with coefficients depending on time and the state.
- The integrand of $J(u^*(t))$ is convex on U and is bounded below by $-c_2 + c_1(u(t))^2$ with $c_1 > 0$.

By definition of U, $\forall$ elements $x \in U, x \in [0,1]$, a closed interval. To prove convexity we show $\forall$ elements $u,\ v \in U,\ u, v \in [0,1]$, any parameterization $\alpha u + (1-\alpha)v$ for any α of a line between any two points in U will remain in U. Since $0 \leq u \leq 1$ and $0 \leq v \leq 1$,

$$0 \leq \alpha u + (1-\alpha)v \leq 1,$$

so $\alpha u + (1-\alpha)v \in U$. All references to state variables in our system of non-linear ordinary differential equations are positive, and the sunlight function $h(t)$ has been defined as periodic and also continuous, but there remains a final unaccounted variable, our traffic function $f(t)$. This $f(t)$ is a piecewise function that is continuous over the course of each hour, and is bounded above and below (see Non-Linear Stability Analysis for definitions of these bounds).

Each concentration is either "constant" ($\overline{O_2}$), a constant rate (k_4), bounded by 1

million (as the concentrations are written in parts per million), or periodic (sunlight, traffic functions) and therefore bounded above by some function or constant. Let

$$J(u(t)) = \int_0^{t_f} \left([NO] + [NO_2] + [CO] + [CO_2] + \frac{\epsilon u^2}{2} \right) dt$$

and recall that

$$U = \{u(t) \; piecewise \; continuous \mid 0 \leq u(t) \leq 1, \forall \in [0, t_f]\}.$$

U is convex if

$$\frac{d^2(J(u(t)))}{du^2} \geq 0$$

$$\frac{d^2}{du^2} \left([NO] + [NO_2] + [CO] + [CO_2] + \frac{\epsilon u^2}{2} \right) = \epsilon$$

Because here $\epsilon > 0$, $J(u(t))$ is convex on U.

By nature our chemical concentrations must be positive, so we have

$$0 \leq [NO], [NO_2], [CO], [CO_2].$$

By definition $u \in [0, 1]$, and it follows that $\frac{\epsilon u^2}{2} \in [0, \frac{\epsilon}{2}]$

$$0 \leq [NO] + [NO_2] + [CO] + [CO_2]$$

$$\frac{\epsilon u^2}{2} \leq [NO] + [NO_2] + [CO] + [CO_2] + \frac{\epsilon u^2}{2}$$

So the integrand is bounded below by $\frac{\epsilon u^2}{2}$.

Thus, we have shown that there exists an optimal method $u(t)$ for our system.

5.2 Determining the Optimal Control

We have examined our proposed policy using optimal control methods for its effectiveness of reducing smog in Los Angeles. In order to employ optimal control, we must first consider where the control would be placed on the equations. In this example, $u(t)$ is the

control function and $J(u(t))$ is the integrand of our functional. We apply our control by multiplying the source term $\alpha_x f(t)$ by the term $(1 - u(t))$. The form of our example

$$\begin{aligned}[\dot{NO}] &= \alpha_{NO} f(1 - u(t)) + h(t) \cdot k_1[NO_2] + h(t) \cdot k_7[HNO_2]^* \\ &\quad -[NO]\left(k_3[O_3] + k_6[NO_2] + k_9[HO_2]^*\right)\end{aligned}$$

can also be applied to any of the other differential equations in our system that are influenced by an emission source term. In our optimal control efforts, we seek to minimize the integral

$$\int_{t_0}^{t_f} ([NO] + [NO_2] + [CO] + [CO_2] + \frac{\epsilon u^2}{2})dt$$

We must determine the Hamiltonian (H) for this system. H is the sum of $J(u(t))$ and the dot product of the left-hand side of the differential equations, and the adjoint functions λ_i. Since we have a system of six differential equations if follows that we will have have six λ_i variables. The Hamiltonian for our study has the form

$$\begin{aligned}H &= [NO] + [NO_2] + [CO] + [CO_2] + \frac{\epsilon u^2}{2} + \lambda_1[\dot{NO}] + \lambda_2[\dot{NO_2}] + \lambda_3[\dot{CO}] \\ &\quad +\lambda_4[\dot{CO_2}] + \lambda_5[\dot{NO_3}] + \lambda_6[\dot{O_3}]\end{aligned}$$

The derivation of a system of adjoint differential equations follows next. We evaluate the partial derivative $\frac{d\lambda_i}{dt}$, which is equal to $-\frac{dH}{dX}$, where X corresponds to a state variable. This results in the system

$$
\begin{aligned}
\frac{d\lambda_1}{dt} &= -\frac{dH}{d[NO]} = -1 - \lambda_1 \left(-\frac{1}{2}\frac{h(t)^2\ k_7^2}{k_6[NO]^2[NO_2]} - k_3[O_3] - k_6[NO_2] \right. \\
&\quad \left. -\frac{k_9\ k_8[CO]\overline{[OH]}}{k_9[NO] + k_{10}[NO_2]} + \frac{[NO]\ k_9^2\ k_8\ CO\ \overline{[OH]}}{k_9\ ([NO] + k_{10} + [NO2])^2} - w \right) \\
&\quad -\lambda_2 \left(k_3\ [O_3] - \frac{k_8\ [CO]\ \overline{[OH]}\ (k_9[NO] - k_{10}[NO_2])\ k_9}{(k_9\ [NO] + k_{10}[NO_2])^2} \right. \\
&\quad \left. + \frac{k_9 k_8[CO]\overline{[OH]}}{k_9[NO] + k_{10}[NO_2]} - k_6\ [NO_2] \right) + \lambda_6 k_3[O_3] \\
\frac{d\lambda_2}{dt} &= -\frac{dH}{d[NO_2]} = -1 - \lambda_1 \left(k_1 h(t) - \frac{1}{2}\frac{h(t)^2 k_7^2}{k_6[NO][NO_2]}[NO] \left(k_6 - \frac{k_9 k_8[CO]\overline{OH} k_{10}}{(k_9[NO] + k_{10}[NO_2])^2} \right) \right) \\
&\quad -\lambda_2 \left(-\frac{k_8[CO]\overline{[OH]}(k_9[NO] - k_{10}[NO_2])k_{10}}{(k_9[NO] + k_{10}[NO_2])^2} - k_1 h(t) - k_4[O_3] - k_6[NO] - k_5[NO_3] - w \right) \\
&\quad -\lambda_3\ (k_4[O_3] - k_4[NO_3]) - \lambda_6(k_1 h(t) - k_4[O_3]) \\
\frac{d\lambda_3}{dt} &= -\frac{dH}{d[NO_3]} = -1 + \lambda_2[NO_2]k_5 - \lambda_3(-[NO_2]k_5 - w) \\
\frac{d\lambda_4}{dt} &= -\frac{dH}{d[CO]} = -1 + \frac{\lambda_1[NO]k_9 k_8\overline{OH}}{k_9[NO] + k_{10}[NO_2]} - \frac{\lambda_2 k_8\overline{OH}(k_9[NO] - k_{10}[NO_2]}{k_9[NO] + k_{10}[NO_2]} - \lambda_4(-k_8\overline{OH} - w) \\
&\quad -\lambda_5 k_8\overline{OH} \\
\frac{d\lambda_5}{dt} &= -\frac{dH}{d[CO_2]} = \lambda_5 w \\
\frac{d\lambda_6}{dt} &= -\frac{dH}{d[O_3]} = (\lambda_1 k_3[NO]) - (\lambda_2(k_3[NO] - k_4[NO_2]) - \lambda_3 k_4[NO_2] \\
&\quad -\lambda_6(-k_3[NO] - k_4[NO_2] - w)
\end{aligned}
$$

In order to be able to solve the adjoint differential equations, the transversality condition $\lambda_i(t_f) = 0$ must be met. Given the transversality condition, we can now solve the adjoint system of differential equations. Following the derivation of the adjoint equations, we seek to find the optimal control function u^*. This is achieved by finding $\frac{\partial H}{\partial u}$ and setting the derivative equal to zero.

$$
\frac{\partial H}{\partial u}|_{u^*} = 0 \Rightarrow u^* = \frac{f(t)(\lambda_1\alpha_1 + \lambda_2\alpha_2 + \lambda_3\alpha_3 + \lambda_4\alpha_4)}{\epsilon} \qquad \text{(-3)}
$$

As can be noticed, the optimal control function is given in terms of λ, which implied that the adjoint equations must be solved in order to use the optimal control function. To solve the systems of differential equations, we employ the Runge-Kutta method of order 4. Using Runge-Kutta, we applied a forward method to the differential equations with state variables and and a backward method for the adjoint equation. The choice in choosing Runge-Kutta as our numerical solver came about when we were comparing solvers between Runge-Kutta and Euler. Numerically, Runge-Kutta is known to be more accurate than the Euler method, however in optimal control, Euler is usually sufficient for numerically solving the differential equations. It was decided that Runge-Kutta would be more appropriate in this situation due to fact that in our system, Runge-Kutta remained as a stable numerical solver.

5.3 Applications of Optimal Control

5.3.1 Policy Proposal

We present an example fuel modification policy: *Beginning January 1, γ% of all registered vehicles in Los Angeles must use exclusively EX fuel in their passenger automobiles or light trucks for the duration of the entire year.*

5.3.2 Figures

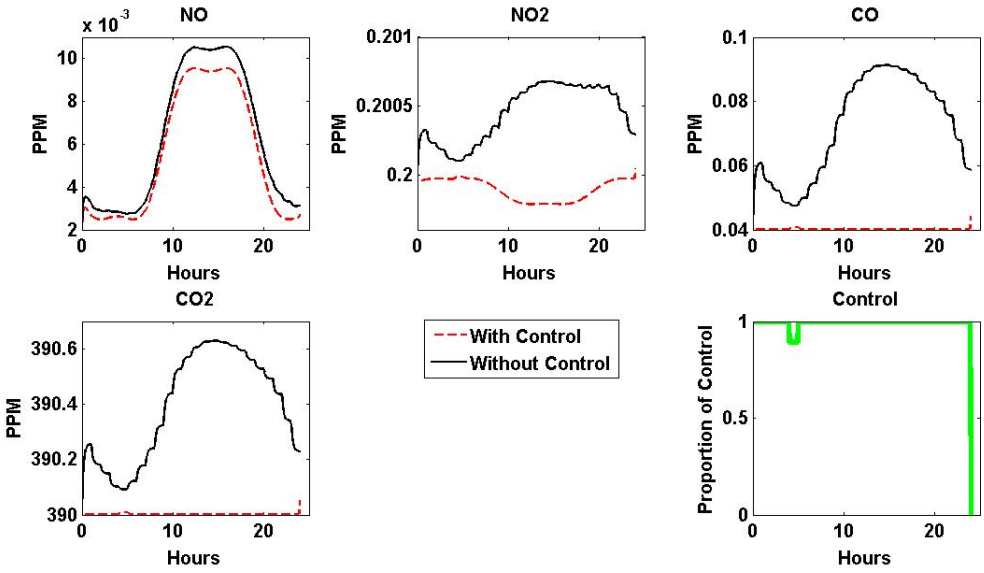

Figure 1: more control, $\epsilon = \frac{1}{9}$,

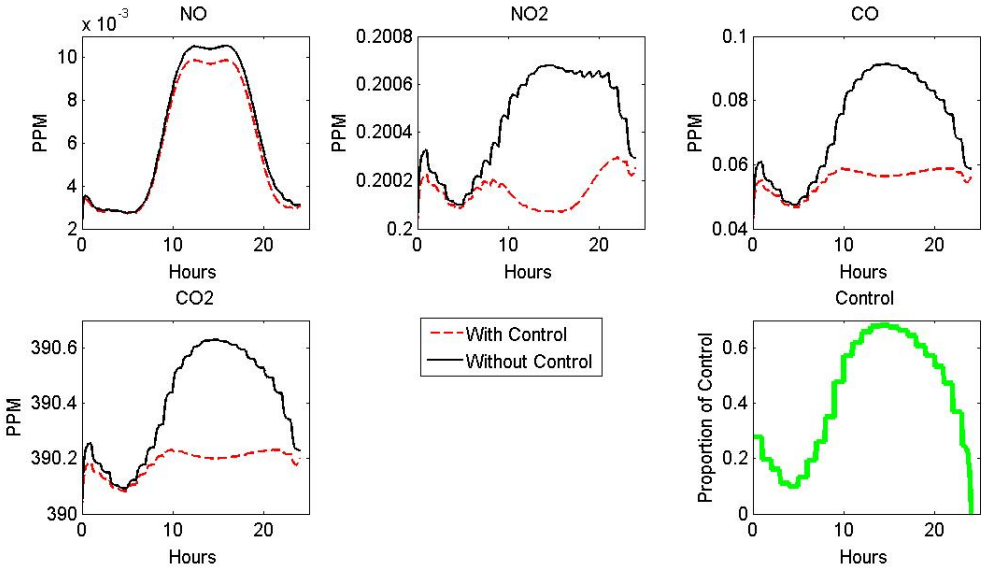

Figure 2: medium control, $\epsilon = \frac{1}{1}$,

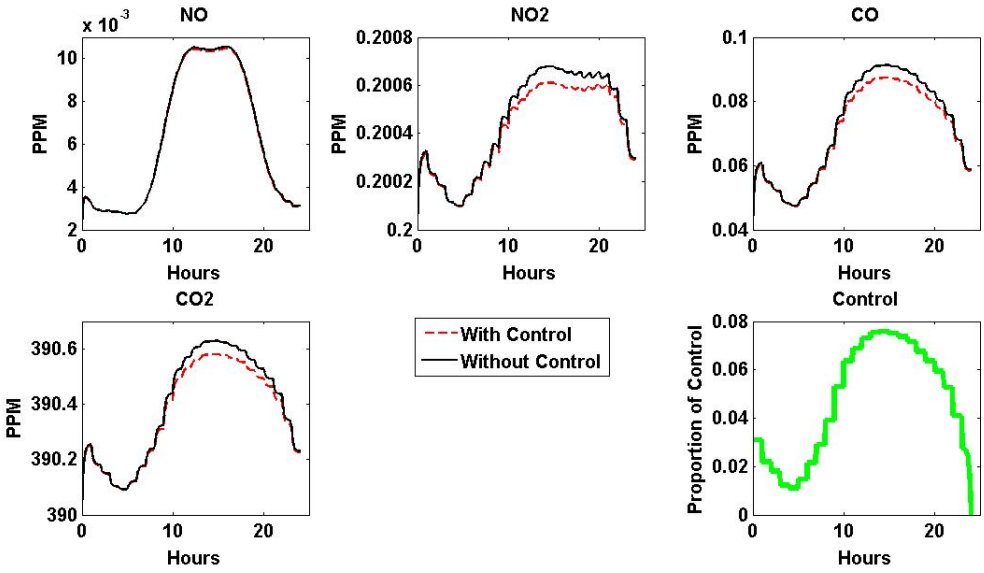

Figure 3: less control, $\epsilon = \frac{9}{1}$,

5.3.3 Example

Given a fixed cost and benefit to implement an E85 policy over a year, suppose a policy maker will only implement a policy if it will yield at least a 1:1 payoff (meaning that for every one dollar invested, the strategy will save one dollar in environmental and health costs), which means that our target $\hat{\epsilon}$ is 1. We have that

$$\hat{\epsilon}(\gamma) = 1 = \frac{\gamma}{100}\frac{cost}{benefit}$$

$$\hat{\epsilon}(\gamma) = 1 = \frac{\gamma\ cars}{100\ cars}\frac{\frac{538{,}835{,}900\ miles}{2{,}499{,}764\ cars{\cdot}year} \cdot \frac{1\ gallon\ E85}{21.1\ miles} \cdot \frac{85\ gallon\ ethanol}{100\ gallons\ E85} \cdot \frac{\$1.78}{1\ gallon\ ethanol}}{\frac{\$37{,}714{,}805.32}{2{,}499{,}764\ cars}}$$

$$100 = \gamma(1.2508)$$

$$\gamma = 79.9488$$

This means that if with the given cost and benefits for the use of E85 fuel, we had a policy where starting January 1 of the coming year, 80% of all registered vehicles in Los

Angeles had to run on E85 exclusively, we would have the maximum amount of control under the condition that we want to (at least) break even financially from the program. We are comparing only the cost of policy implementation and maintenance versus reduction in health cost. We could also expect the behavior of the pollutant concentrations to behave like Figure 3 above, if the time on those graphs were extended to span a year.

5.3.4 Example

This γ strategy could also apply if a policy maker already knows that they will only be able to reach a certain percent of all registered vehicles with a policy. For example, suppose our E85 policy were not legally enforced, but rather suggested. Also suppose that for a suggested policy, we can only expect a 60% response rate from the population. We can then calculate the relative $\hat{\epsilon}$

$$\hat{\epsilon}(60) = \frac{60}{100}\frac{cost}{benefit}$$

$$\hat{\epsilon}(60) = \frac{60\ cars}{100\ cars}\frac{\frac{538{,}835{,}900\ miles}{2{,}499{,}764\ cars \cdot year} \cdot \frac{1\ gallon\ E85}{21.1\ miles} \cdot \frac{85\ gallon\ ethanol}{100\ gallons\ E85} \cdot \frac{\$1.78}{1\ gallon\ ethanol}}{\frac{\$37{,}714{,}805.32}{2{,}499{,}764\ cars}}$$

$$\hat{\epsilon}(60) = \frac{60}{100}(1.2508)$$

$$\hat{\epsilon}(60) = .75048$$

So for a supposed E85 plan where only 60% of all drivers will comply with the policy, the relative cost will be approximately $\frac{3}{4}$. Incorporating this $\hat{\epsilon}$ value into the control function will yield more accurate results from optimal control.

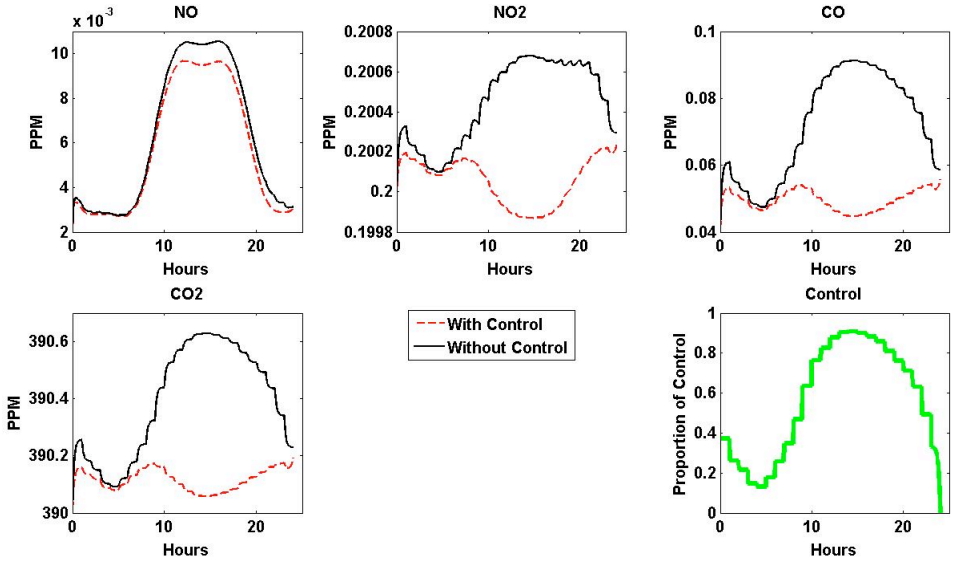

Figure 4: control when $\epsilon = .75048$

6 Discussion and Summary

We were able to construct a system that describes the chemical relationships between each compound of photochemical smog while also considering external emission sources and detractors. Our team is not the first to approach the causes or effects of photochemical smog, but we noticed a void of information connecting the physical characteristics of the smog components to any type of implementable policy. Our particular goal was to fill this gap, providing a framework upon which policy makers could build a strategy of human intervention to combat global warming and air pollution in Los Angeles. What sets our study apart from our predecessors is the incorporation of optimal control into the system. We neglect neither the physical nor the financial realities of the Los Angeles smog crisis, ensuring that our policy suggestions are both physically possible and economically responsible.

The effectiveness of enforcing an ethanol/petroleum fuel policy depends on which environmental problem is of greater concern. We have considered the formation processes of both carbon dioxide and ozone, which contribute to long-term global warming and short-term health effects, respectively. Our simulations show that the optimal control function we have developed has a noticeable effect on carbon dioxide levels, but little to no effect on ozone levels. This suggests that if reducing ozone levels is the priority, an ethanol policy may not be worth the financial investment.

A conundrum presented by Los Angeles air pollution is whether to first address ozone levels (which are immediately perceptible and decrease the standard of living of those who interact with it) or carbon dioxide emissions (the effects of which will result from a gradual accumulation in the atmosphere). This becomes a "short-term versus long-term" problem. When considering carbon dioxide emissions, catalytic converters may be called into question. These emission controls, mandatory for non-commercial vehicles and illegal to tamper with, convert carbon monoxide to carbon dioxide within the engine. The theory behind catalytic converters is to reduce the immediate emission of poisonous carbon monoxide gas, but this comes at the cost of increasing carbon dioxide emission.

Of the chemicals in our study, ozone poses a unique problem: in a 1993 study Seinfeld et. al. supposed that even if all auto emissions were eliminated by 2010, ozone concentrations would only be approximately 10% lower than they would be if no reduction plan were implemented, [6], a result which our study reinforces. Because the differential equation for ozone contains no $\alpha_x f(t)$ source term, we know that the production of ozone comes primarily from photochemical reactions of other molecules and that ozone formation is not influenced directly by vehicular emissions. The lack of a vehicular source term for ozone means that we do not apply our optimal control function $u(t)$ directly to the ozone differential equation. Therefore, any control we impose on the system will immediately result in little direct change to either ozone or NO_3, which is in a similar situation.

Despite advancements in vehicular emission controls, the massive increase in commuters over the last five decades has perpetuated the issue of photochemical smog in Los Angeles. Our simulations have shown that displacement (wind) and sink (plant and soil) factors are not sufficient to counter the accumulation of smog-forming chemicals that are emitted by automobiles.

6.1 Smog Checks

Even if such an ethanol policy were rigorously and comprehensively executed, it may not make much of a dent in the emission problem. Another roadblock to environmental clarity is the fraction of vehicles on the roads that the state of California would classify as "dirty". These cars and trucks, less than 10% of traffic, contribute over 50% of all vehicular emissions, [18]. Although they would fail smog tests for various reasons, "dirty" vehicles remain on the roads. This is due in part to a failure of the California Smog Check program. An undercover study found that smog stations sometimes take bribes to pass undeserving cars, are unable to fix dysfunctional control devices, and fail to diagnose problems with the cars, [18]. Investing more research and funding toward improving the Smog Check program may prove to be a worthwhile endeavor.

6.2 Future Work

Research into the temporary closure of the I-405 highway in Los Angeles, also known as "Carmageddon", should be conducted in order to determine its effect on health and air pollution. A fortunate and predictable consequence of the closure was that as traffic density decreased, air pollution levels declined. A more in-depth analysis of Carmageddon's impact on health and air pollution in Los Angeles should be conducted. A related and more general field of future study might be finding an optimal policy specifically regarding the control of traffic behavior.

7 Acknowledgements

We thank Dr. Carlos Castillo-Chavez, Mr. Benjamin Morin, and Professor Sunmi Lee for support, valuable discussions and encouragement. A thank you from Arturo Vargas goes to Rosie Leung and Dustin Padilla who showed that Mathematics will always be a stimulating field. This research is supported in part by the National Science Foundation–Enhancing the Mathematical Sciences Workforce in the 21st Century (EMSW21), award #0838705; the Alfred P. Sloan Foundation–Sloan National Pipeline Program in the Mathematical and Statistical Sciences, award #LTR 05/19/09; and the National Security Agency–Mathematical & Theoretical Biology Institute—Research Program for Undergraduates; award #H98230-09-1-0104.

References

[1] Atkinson, S. E., Lewis, D. H.; *A Cost-Effective Analysis of Alternative Air Quality Control Strategies*, Journal of Environmental Economics and Management, 1974.

[2] Bailey, Clark, Ferris, Krause, Strong; *Chemistry of the Environment*, Second Edition, Harcourt/Academic Press, 2002.

[3] Becker, R., Kapp, H., Rannacher, R.; *Adaptive Finite Element Methods for Optimal Control of Partial Differential Equations*, SIAM Journal of Control and Optimization, 2001.

[4] Bourne, J.K.; *Green Dreams*, National Geographic, 2007. `http://ngm.nationalgeographic.com/2007/10/biofuels/biofuels-text/1`.

[5] California Department of Transportation; *Caltrans Performance Measurement System (PeMS)*, 2011.

[6] Calvert, J. G., Heywood, J. B., Sawyer, R. F., Seinfeld, J. H.; *Achieving Acceptable Air Quality: Some Reflections on Controlling Vehicle Emissions*, Science Magazine, Volume 261, 1993.

[7] Center for Sustainable Systems; *Personal Transportation*, University of Michigan, 2010. `http://css.snre.umich.edu/css_doc/CSS01-07.pdf`.

[8] Clean Up Green Up *Toxic Overload in LA's Low-Income Communities of Color*, `http://cleanupgreenup.wordpress.com/resources-2/`.

[9] Consumer Reports; *The great ethanol debate*, 2011. `http://www.consumerreports.org/cro/cars/new-cars/news/ethanol/overview/index.htm`

[10] de Pillis, L. G., Gu, W., Fister, K. R., Head, T., Maples, K., Murugan, A., Neal, T., Yoshida, K.; *Chemotherapy for tumors: An analysis of the dynamics and a study of quadratic and linear optimal controls*, 2006.

[11] Energy Future Coalition; *The Benefits of Biofuels: Environment and Public Health*, 2007. http://www.energyfuturecoalition.org/biofuels/graphs/benefits/ph_graph2.htm.

[12] Environmental Protection Agency; *E85 and Flex Fuel Vehicles: Technical Highlights*, 2010. http://www.epa.gov/otaq/renewablefuels/420f10010.pdf.

[13] Environmental Protection Agency; *Clean Air Act*, 2011.

[14] Environmental Protection Agency; Emission Facts: Average Annual Emissions and Fuel Consumption for Passenger Cars and Light Trucks, 2000. http://www.epa.gov/oms/consumer/f00013.htm

[15] Foust, R.; *Photochemical Smog*, http://mtweb.mtsu.edu/nchong/Smog-Atm1.htm.

[16] Fuel Flex International; International Store, 2011

[17] GasBuddy.com; *Average Gas Prices in Los Angeles*, 2011.

[18] Glazer, A., Klein, D. B., Lave, C.; *Clean on Paper, Dirty on the Road: Troubles with California's Smog Check*, 1995. http://www.jstor.org/stable/pdfplus/20053062.pdf?acceptTC=true.

[19] Hale, J., Kocak, H.; *Dynamics and Bifurcations*, Springer-Verlag, 1991.

[20] Husar, R. B., White, W. H.; *On the Color of Los Angeles Smog*, Atmospheric Environment, 1976.

[21] Inman, R. E., Ingersoll, R. B., Levy, E. A.; *Soil: A Natural Sink for Carbon Monoxide*, Science, New Series, 1971.

[22] Jorgenson, A. K., Kick, E. L.; *Globalization and the Environment*, 2003.

[23] Lenhart, S., Workman, J T.; *Optimal Control Applied To Biological Models*, Chapman and Hall/CRC, 2007.

[24] Los Angeles Almanac; *Number of Days Exceeding Federal & State Air Quality Standards per Year: Los Angeles County*, 2008.

[25] Los Angeles County Department of Public Health; *Health Impacts of Air Pollution in Los Angeles County*, 2007.

[26] Los Angeles Department of Transportation; *The City of Los Angeles Transportation Profile*, 2009. `http://ladot.lacity.org/pdf/PDF10.pdf`.

[27] McRae, G. J., Goodin, W. R., Seinfeld, J. H.; *Development of a Second-Generation Model For Urban Air Pollution: I. Model Formulation*, Atmospheric Environment, 1981.

[28] Meier, F.; *EPA allows 15% ethanol in gasoline, but only for late-model cars*, USA Today, 2010.

[29] Milford, J. B., Russell, A. G., McRae, G. J.; *A new approach to photochemical pollution control: implications of spatial patterns in pollutant responses to reductions in nitrogen oxides and reactive organic gas emissions*, Environ. Sci. Technol., 1989.

[30] Mishra, V.; *Health Effects of Air Pollution*, Minnesotans for Sustainability, `http://www.mnforsustain.org/climate_health_effects_of_air_pollution_mishra_pern.htm`, 2003.

[31] Munroe, Tapan; Schmidt, Ronald; Westwind, Mark, *Economic Benefits of Toll Roads Operated by the Transportation Corridor Agencies*, LECG, 2006, https://www.thetollroads.com/home/images/publications/6_15_06_LeCG_Toll_Road_Study.pdf.

[32] Nadler, Johnathan; Traffic Congestion and Air Quality, SCAG, 2007. http://www.scag.ca.gov/factsheets/pdf/2007/traffic07.pdf.

[33] Phillips, Kathryn, *Reducing Global Warming and Air Pollution: The Role of Green Development in California*, 2008, http://www.environmentnow.org/pdf/Summary-of-Larry-Frank-Paper-on-ISR-and-GHG.pdf.

[34] Pidwirny, M.; *Atmospheric Effects on Incoming Solar Radiation*. Fundamentals of Physical Geography, 2nd Edition, http://www.physicalgeography.net/fundamentals/7f.html, 2006.

[35] Pidwirny, M.; *Earth-Sun Relationships and Insolation*. Fundamentals of Physical Geography, 2nd Edition. http://www.physicalgeography.net/fundamentals/6i.html, 2006.

[36] Pike, Ed; *Congestion Charging: Challenges and Opportunities*, The International Council on Clean Transportation, 2010, http://www.theicct.org/pubs/congestion_apr10.pdf.

[37] Pitts, Jr., J. N., Atkinson, R., Winer, A. M.; *Formation and Fate of Toxic Chemicals in California's Atmosphere*, California Air Resource Board, 1984.

[38] Rattner, S.; *The Great Corn Con*, The New York Times, 2011.

[39] Reynolds, S., Roth, P. M., Seinfeld, J. H.; *Mathematical Modeling of Photochemical Air Pollution*, Atmospheric Environment, 1973.

[40] Romley, John A., Andrew Hackbarth and Dana P. Goldman. *The Impact of Air Quality on Hospital Spending*. Santa Monica, CA: RAND Corporation, 2010. `http://www.rand.org/pubs/technical_reports/TR777`.

[41] Samaras, C., Meisterling, K.; *Life Cycle Assessment of Greenhouse Gas Emissions from Plug-in Hybrid Vehicles: Implications for Policy*, Carnegie Mellon, Environ. Sci. Technology, 2008.

[42] Segel, L. A., Slemrod, M.; *The Quasi-Steady-State Assumption: A Case Study in Perturbation*, SIAM Review, 1989.

[43] Seinfeld, J. H., Hecht, T. A., Roth, P. M.; *A Kinetic Mechanism for Atmospheric Photochemical Reactions: Development of a Simulation Model for Estimating Ground Level Concentrations of Photochemical Pollutants*, EPA, 1971.

[44] Smith, M. T.; *Fact Sheet: Exhaust System Repair Guidelines*, EPA, 1991. `http://www.epa.gov/compliance/resources/policies/civil/caa/mobile/exhsysrepair.pdf`.

[45] Sontag, E. D.; *Lecture notes on mathematical systems biology* Lecture notes, Rutgers University, New Brunswick, New Jersey, October 2010.

[46] Su, F.; *The Concern Over Anthropogenic Air Pollution*, University of California at Berkeley, `http://are.berkeley.edu/courses/EEP101/spring03/AllThatSmog/back.html`, 2002.

[47] Sullivan, Edward; Burris, Mark; *Benefit-Cost Analysis of Variable Pricing Projects: SR-91 Express Lanes*; Journal of Transportation Engineering, 2006.

[48] Sun, J., Sivashankar, N.; *An application of optimization methods to the automotive emissions control problem*, American Control Conference, 1997.

[49] *The Chemistry of Photochemical Smog*, http://www.freewebs.com/bmstmt/Tieng%20anh/THE%20CHEMISTRY%20OF%20PHOTOCHEMICAL%20SMOG.pdf.

[50] Time and Date, *Sunrise and Sunset in Los Angeles*, http://www.timeanddate.com/worldclock/astronomy.html?n=137.

[51] Trijonis, J. C.; *Economic air pollution control model for Los Angeles County in 1975*, Environ. Sci. Technol., 1974.

[52] U. S. Census Bureau; *Los Angeles County QuickFacts*, 2011.

[53] Verwer, J. G., van Loon, M.; *An Evaluation of Explicit Pseudo-Steady-State Approximation Schemes for Stiff ODE Systems from Chemical Kinetics*, Stichting Mathematisch Centrum, 1993

[54] Wiesenfelder, J.; *E85: Will it Save You Money?*, Cars.com, 2010. http://www.cars.com/go/advice/Story.jsp?section=fuel&subject=fuelAlt&story=e85.

8 Appendix

Table 1: Generalized reactions of photochemical smog

$NO_2 + hv \xrightarrow{k_1} NO + O$
$O + O_2 + M \xrightarrow{k_2} O_3 + M$
$O_3 + NO \xrightarrow{k_3} NO_2 + O_2$
$O_3 + NO_2 \xrightarrow{k_4} NO_3 + O_2$
$NO_3 + NO_2 \xrightarrow{k_5} 2HNO_3$
$NO + NO_2 \xrightarrow{k_6} 2HNO_2$
$HNO_2 + hv \xrightarrow{k_7} OH + NO$
$CO + OH \xrightarrow{k_8} CO_2 + HO_2$
$HO_2 + NO \xrightarrow{k_9} OH + NO_2$
$HO_2 + NO_2 \xrightarrow{k_{10}} HNO_2 + O_2$
$HC + O \xrightarrow{k_{11}} \alpha RO_2$
$HC + OH \xrightarrow{k_{12}} \beta RO_2$
$HC + O_3 \xrightarrow{k_{13}} \gamma RO_2$
$RO_2 + NO \xrightarrow{k_{14}} NO_2 + \epsilon OH$
$RO_2 + NO_3 \xrightarrow{k_{15}} PAN$

Table 2: Base values of reaction rate constants

$k_1 = 0.266\ min^{-1}$
$k_2 = 2.76 \times 10^6\ min^{-1}$
$k_3 = 21.8\ ppm^{-1}min^{-1}$
$k_4 = 0.006\ ppm^{-1}min^{-1}$
$k_5 = 0.1\ ppm^{-1}min^{-1}$
$k_6 = 5 \times 10^{-4}\ ppm^{-1}min^{-1}$
$k_7 = 5 \times 10^{-3}\ min^{-1}$
$k_8 = 1.8 \times 10^3\ ppm^{-1}min^{-1}$
$k_9 = 1.8 \times 10^3\ ppm^{-1}min^{-1}$
$k_{10} = 10\ ppm^{-1}min^{-1}$
$k_{11} = 7300\ ppm^{-1}min^{-1}$
$k_{12} = 9500\ ppm^{-1}min^{-1}$
$k_{13} = 1.9 \times 10^{-3}\ ppm^{-1}min^{-1}$
$k_{14} = 1.8 \times 10^3\ ppm^{-1}min^{-1}$
$k_{15} = 13.8\ ppm^{-1}min^{-1}$

Table 3: Percentage increase from initial conditions for specific species

Pollutant	% increase	Mean	Standard Deviation
NO_2	100.59	0.2004	0.0003
NO	867.47	0.0087	0.0046
O_3	197.21	0.0006	0.0001
CO	236.55	0.0739	0.0162
CO_2	100.17	390.4165	0.1990